

The Remarkable Be Star HD110432 (BZ Cru)

Myron A. Smith

*Catholic University of America,
3700 San Martin Dr., Baltimore, MD 21218;
msmith@stsci.edu*

and

Luis Balona¹

*South African Astronomical Observatory,
P. O. Box 9, Observatory 7935, South Africa;
lab@sao.ac.za*

ABSTRACT

HD 110432 (B1e) has gained considerable recent attention because it is a hard, variable X-ray source with local absorption and also because its optical spectrum is affected by an extensive Be disk. From time-serial echelle data obtained over two weeks during 2005 January and February, we have discovered several remarkable characteristics in the star's optical spectrum. The line profiles show rapid variations on some nights which can most likely be attributed to irregularly occurring and short-lived *migrating subfeatures*. Such features have been found in spectra of γ Cas and AB Dor, two stars for which it is believed magnetic fields force circumstellar clouds to corotate over the star's surface. The star's optical spectrum also exhibits a number of mainly Fe II and He I emission features with double-lobed profiles typical of an optically thin circumstellar disk viewed nearly edge-on. Using spectral synthesis techniques for the January data, we find that its temperature and column density are close to 9,800 K and roughly $3 \times 10^{22} \text{ cm}^{-2}$. Its projected disk size covers a remarkably large 100 stellar areas, and the emitting volume resides at a surprisingly large distance of 1 A.U. from the star. Surprisingly, we also find that the absorption wings of the strongest optical and UV lines in the spectrum extend to at least $\pm 1000 \text{ km s}^{-1}$, even though the rotational velocity is 300–400 km s^{-1} . We are unable to find a satisfactory explanation for these extreme line broadenings. Otherwise, HD 110432 and

γ Cas share similarly peculiar X-ray and optical characteristics. These include as high X-ray temperature, erratic X-ray variability on timescales of a few hours, optical metallic emission lines, and submigrating features in optical line profiles. Because of these similarities, we suggest that HD 110432 is a member of a select new class of “ γ Cas analogs.”

Subject headings: :

stars: individual (HD 110432) – stars: individual (γ Cas) – stars: emission-line, Be –
ultraviolet: stars – X-rays: stars

1. Introduction

HD 110432 (BZ Cru = HR 4830, $m_v = 5.3$) is a bright variable late-Oe to Be-type star (Houk & Cowley 1975) located in the open cluster NGC 4609 (Feinstein & Marraco 1979) and beyond the southern Coalsack. In recent years this star has attracted considerable attention, resulting in several investigations in the X-ray, ultraviolet, and optical wavelength regimes. In each regime, the star has been found to be unusual. The optical spectrum is distinguished by Balmer and Fe II lines having double-lobed emission profiles (Slettebak 1982), which is an unusual attribute for classical Be stars. Because the optical spectrum does not show forbidden Fe lines, nebular lines, or features due to a cool companion, it fails the definition of a B[e] star. The star’s substantially reddened colors and linear polarization have made it an important candidate for ultraviolet and optical for studies of interstellar extinction. In this respect the star’s reddening is unusual and suggests that its observed flux distribution has been altered by circumstellar matter (Meyer & Savage 1981).

In their classic X-ray survey of potential Be X-ray binary systems, Torrejón & Orr (2001, hereafter TO01) found that HD 110432 is a hot thermal X-ray source. Its light curve, extracted from BeppoSax spectra, does not show rapid pulses ($\leq 10^3$ sec) characteristic of a Be X-ray pulsar system, transients, or alternating extended high and low states that are typical of most Galactic X-ray Be stars (and CV systems). These authors found that the spectrum can be fit with a MEKAL model with a temperature of $kT = 10.55$ keV or with a power law fit with a photon index $\alpha = 1.35$ and cut-off energy $E_c = 16.69$ keV. The power-law fit may be improved by the addition of Fe 6.7 and 6.9 keV emission lines. However, since the presence of these lines is consistent with the slope of the X-ray continuum, a thermal interpretation is to be preferred. The absorption column density from the attenuation of soft X-ray continuum flux in this model is about 1.08×10^{22} cm $^{-2}$, or fully a factor of ten higher than the ISM column densities inferred from ultraviolet atomic and molecular hydrogen lines (Rachford et al. 2001).

TO01 extracted a 5-hour light curve from their BeppoSax observations and discovered that it was characterized by a 4-hour modulation. TO01 supposed that the variation in this light curve is periodic and ascribed it to a 4-hour rotation of a hypothetical white dwarf with a spotted surface in a binary system. Because modulations on this timescale are common in the light curve of γ Cas (Robinson, Smith, & Henry 2002, hereafter RSH02) and since an X-ray temperature of $\approx 10^8$ K (10.55 keV) is also characteristic, of γ Cas (e.g., Owens et al. 1999, Smith et al. 2004), the TO01 study suggested that follow-up observations on HD 110432 would be productive to establish whether it showed the optical light curve and spectroscopic attributes of γ Cas as well.

Our discussion in this paper proceeds by first describing the observational and modeling

tools (§2) used in the analysis and reviewing the known fundamental parameters of the HD 110432 (§3). We then explore the star’s known X-ray and optical light curves (§4) and the properties of archival UV resonance line (§5) and newly obtained optical spectra (§6). In §7 we outline the likely properties of members of a “ γ Cas” class of stars.

2. Observations and Modeling Tools

2.1. Optical data

In this study we obtain photometric and spectroscopic observations of HD 110432 to investigate whether its optical properties might be related to the X-ray variability. The photometric observations were carried out by the observing staff of the 0.5-m telescope at African Astronomical Observatory’s Sutherland station during 2002 February 6–May 7 in the Cousins V and B filters. The comparison stars used for these observations were two late-type B stars, HR 4736 and HR 4944. All three stars were observed through the same neutral density filter and standardized with respect to “E-region” UBVRI photometric standards.

To investigate the properties of the disk and the star’s optical variability over short time scales, we undertook a high resolution spectroscopic campaign during February 2005. Using the fiber-fed *Giraffe* spectrograph attached to the 1.9-m telescope of the South African Astronomical Observatory (SAAO). This echelle spectrograph is a copy of the MUSICOS spectrograph of the Telescope Bernard Lyot at Pic du Midi Observatory (Baudrand & Bohm 1992). The configuration places 50 spectral orders on a 1024×1024 TEK CCD detector covering the range $\lambda\lambda 4270$ – 6800 . The spectral resolution was 32,000, and the dispersion ranged from 0.06 – $0.09 \text{ \AA pixel}^{-1}$. A Th–Ar arc lamp was used to provide a wavelength calibration, with arc spectra being taken at regular intervals to minimize instrumental drift. Flatfielding was accomplished by illuminating the camera with uniform light provided by a tungsten filament lamp and diffusing screen. Echelle blaze functions were determined by measuring the response across each order when the fiber was illuminated by the tungsten lamp. This procedure was largely (but not completely) effective in rectifying the continuum. The data reduction was carried out using the “SPEC2” spectroscopic data reduction package, as used by most other observers of this instrument.

We obtained 142 spectra during on the nights of 2005 January 26 –February 1. Dr. David Laney kindly obtained 61 additional spectra for us on February 22–March 1, 2005. Typically we obtained a signal-to-noise ratio of 50 per pixel in an exposure time of 10–20 minutes. Nine of the fifteen nights were suitable for a search for *migrating subfeatures*, which are discussed below, according to our (somewhat arbitrary) criterion of at least 10

observations distributed over at least three hours on a given night.

In order to place the continuum in an objective a manner, we first constructed a synthetic spectrum with similar effective temperature and gravity. The lines were then broadened for the appropriate rotational velocity. We then found the ratio between the observed and synthetic spectrum and selected those points which are on the continuum, according to the synthetic spectrum. This step involves filtering and smoothing. Finally, a low-order polynomial (usually of degree 3) was fitted to the observed points on the spectrum deemed to be on the continuum. This procedure is completely automatic and has been used in all observations of early-type stars made with *Giraffe*. Comparison between the observed spectrum and the synthetic spectrum is always very good except for the region around the Balmer lines.

2.2. Spectral synthesis modeling

In §6.2.2 we will discuss results of a number of line syntheses we performed using the *SYNSPEC* code, version 48, written by Hubeny, Lanz, and Jeffery (1994). As input for these solutions, we used the atomic data from the line library (Kurucz 1990) and a standard model atmosphere (Kurucz 1990) having parameters $T_{\text{eff}} = 25,000$ K, $\log g = 4$, and $\xi = 2$ km s⁻¹. Our synthesized spectra were computed in steps of 0.01 Å. We assumed standard abundances for these computations and convolved the result with an Unsold “rotation function” using computed continuum intensities determined for a grid of 20 μ angles from a vertical direction in the atmosphere. To compute the effect of a circumstellar “cloud” or disk on the spectrum we used the output from our *SYNSPEC* calculation as input for a computation of cloud absorption or emission by the *CIRCUS* program (Hubeny & Heap 1996).

In both these programs we used a working value of $V_{\text{rot}} \sin i = 300$ km s⁻¹ as determined in §3. However, this value need not be known precisely because the narrower emission line contributions can be easily separated from the underlying broad photospheric line absorptions. We ran *CIRCUS* in its LTE reemission mode, that is, by evaluating the radiative transfer relations assuming a locally defined excitation and ionization temperature. Other important disk physical parameters used to compute the equivalent widths of lines formed in the disk are its column density, projected disk area, microturbulence, and chemical composition (assumed herein to be solar). A volumetric particle density of 1×10^{12} cm⁻³ was chosen from the disk model for γ Cas (Millar & Marlborough 1998; their Table 1). This density corresponds to a point one scale height out of the disk plane and about $1R_*$ from the star’s surface. *CIRCUS* handles as many as three clouds with independent velocity and thermodynamic parameters. Except in one case, we imposed the condition that our model

disks were homogeneous. For the exception as noted below, we utilized this capability and constructed a two-temperature disk model.

In many such applications, one has to make educated guesses to set the most important parameter, the disk temperature. In this paper we will be able to provide an accurate determination of the temperature by the simultaneous presence of iron and helium line strengths in the disk spectrum. The temperature guess drives our values of other parameters. Another important determination is the regime of optical depth (thick or thin?) through which the lines are observed. The equivalent width ratios of iron lines having different atomic gf values enable one to estimate the optical depths and the hence column densities of the disk region. However, we should emphasize in advance that while these properties define the total volume of the emitting gas, they do not define its distance from the exciting star or the internal density distribution. These conditions are better defined by separate kinematic arguments.

3. Fundamental physical properties of HD 110432

Observations of HD 110432’s optical and UV spectrum suggest a spectral type in the range of B0.5 to B2 (Hiltner et al. 1969, Codina et al. 1984, Ballereau, Chauville, & Zorec 1995). Although previous distance estimates have run as high as 430 ± 60 pc (Codina et al. 1984), *Hipparcos* parallaxes have led to a more modest value of 300 ± 50 pc (Perryman 1997).

Surveys of OB stars have determined that the UV reddening curve of HD 110432 is peculiar (e.g., Meyer & Savage 1981). In their summary of E(B-V) reddening results for this star in the literature, Rachford et al. (2001) concluded that a “low” value of $E(B-V) = 0.40$ magnitudes results if the star’s parameters lies within the spectral type and class ranges of B0–B2 and V-III, respectively, if the *Hipparcos* parallax is correct within its errors, and if the reddening toward the star is representative of the average Galactic relation. One can reconcile this low E(B-V) with the value of 0.51 found by Meyer & Savage if one attributes a reddening difference $\Delta E(B-V) \approx 0.11$ to a circumstellar nebula or disk near the star.

Zorec, Frémat, & Cidale (2005) have recently calibrated the Balmer jump criteria (D, λ_1) they measure in 97 OB stars to current-generation model atmospheres. This work allowed them to assign values of $T_{\text{eff}} = 22,510$ K and $\log g = 3.9$ to HD 110432. However, we have found that the strengths of certain UV temperature-sensitive lines indicate a slightly higher temperature. For example, the HeII $\lambda 1640$ line is almost as strong (90–95%) as in the γ Cas spectrum. In addition, Codina et al (see their Fig. 1) determined parameters $T_{\text{eff}} = 25,000$ K and $\log g = 3.5$ from a UV-to-near-IR fitting of the star’s spectral energy distribution

with models computed from model atmospheres. We have adopted the Codina et al. value for our line syntheses. This is slightly cooler than most estimates of the T_{eff} for γ Cas, and so we adopt a spectral type of B1 IV.

The radial velocity of HD110432 is uncertain because its few strong absorption lines are very broad. An examination of the literature shows determinations ranging from +9 to +35 km s^{-1} . Because of this scatter, the star is generally noted as being variable in velocity, and this is probably due to emission of its blue lines for at least some decades. For example, we note the comment by Thackeray, Tritton & Walker (1973; TTW73): “The H emission lines are very strong, being visible at least as far as H9. The velocities are mainly based on Balmer emission. He absorption is faintly visible (B8 V) and Fe II emission suspected.” We have adopted for this study the most recently determined value of +9 km s^{-1} by TTW73.

According to the literature, the rotational velocity of HD 110432 has been obtained from either the $\lambda\lambda 4471\text{--}4481$ optical region or the UV resonance lines. In the first case, various optical studies have attempted to measure the $V_{\text{rot}} \sin i$ from the He I 4471 Å line. (The often used nearby Mg II 4481 Å line is hopelessly blended in this star’s spectrum.) These studies have given results in the range of 300–380 km s^{-1} (Slettebak 1982, Ballereau, Chauville, & Zorec 1995). However, the latter authors believed that this line was probably mutilated at the time of their observation (Zorec 2005). In light of our new data (see §6.3), we believe that any velocities derived from fitting this this line are open to question. Codina et al. (1984) were able to fit the CIV and Si IV resonance lines with a broadening parameter of of 360 km s^{-1} that they attributed to rotation. However, as we will develop below, there appears to be an issue as to whether the components these authors identified are photospheric. In view of these uncertainties, we display in Figure 1 the $\lambda\lambda 1115\text{--}40$ region of the FUSE spectrum, as obtained from the MAST archives. In this figure we have fit the observed spectrum with a synthetic spectrum computed with *SYNSPEC* using a rotational parameter $V_{\text{rot}} \sin i = 300$ km s^{-1} with an 5% emission component from a warm (20,000 K) circumstellar cloud. The *FUSE* spectra of HD 110432 and γ Cas in this spectral region exhibit essentially the same broadening. We have also performed a similar exercise for the fitting of the He II 1640 Å line, as shown in Figure 2, and for the Fe III line-rich region of $\lambda\lambda 1910\text{--}1930$ (not shown). We found a good fit to the line profiles with $V_{\text{rot}} \sin i = 300$ km s^{-1} in both cases. While these rotational velocity determinations are internally consistent, they are at the low end of the 300–380 km s^{-1} range quoted above from fitting of optical lines. The disparity with our result is an example of a well-known tendency of UV line analyses to result in lower rotational velocities than analyses of optical lines. We believe that optical determinations should be preferred over our own because the nearby continuum can be placed with more confidence. For example, we find that a rise in the fluxes in the $\lambda\lambda 1637\text{--}1638$ region, probably a true continuum reference window, is not easily matched in our syntheses of spectra of several

other early-type Be stars. In addition, it is likely that gravity darkening in these very rapidly rotating stars deemphasizes the contribution of lines formed near the equator. Such lines would be formed at higher latitude regions where the total range of local rotational velocities is smaller. A convincing demonstration of this principle was shown in the case of the rapidly rotating star ζ Oph by Reid et al. (1993). These authors noted the absence of line profile variations due to equatorially confined nonradial pulsations in high-excitation lines of He II and N III, while lines of less excited ions showed variations from the equatorial mode. The most important result to take away from this work is that the velocity is probably *at least* 300 km s^{-1} . Whatever the precise value is, Fig. 1 shows that it is likely nearly the same as the velocity of γ Cas.

4. Light Curve Modulations

4.1. The X-ray light curve of Torrejón and Orr

By kind permission of J. Torrejón, we have reproduced the BeppoSax light curve published by TO01 as Figure 5. Their light curve shows a dip in X-ray flux followed about two hours later by a rise to the initial flux. Although TO01 suggested that the variation in this light curve is periodic, a single cycle leaves open the possibility that its variations can be characterized in other ways. To show how another interpretation is possible, we depict in Figure 4 an *RXTE* light curve of γ Cas over a comparable stretch of time. This particular time sequence was taken from that shown by Figure 2 of Robinson & Smith (2000), and it is centered at about 10 UT on 1998 November 24. Superimposed on this figure is the sine curve fit obtained by TO01 for the HD 110432 data, adjusted for count rate. Clearly, the TO01 sine wave for HD 110432 is a good fit to the γ Cas variations. Yet, a glance at the full data train in the Robinson & Smith figure makes it obvious that “sinusoidal variation” in the γ Cas curve is actually part of a series of a seemingly random meandering pattern that suggest that the appearance of a periodicity is illusory. From this comparison the temporal characteristics of the light curves of HD 110432 and γ Cas are essentially the same.

4.2. Optical cycles?

Because both the X-ray temperature and variability properties of HD 110432 are reminiscent of γ Cas, we decided to look for other possible similarities in terms of published X-ray/optical correlations.

We began our optical study of HD 110432 by a photometric monitoring campaign in

2002. This followed the report by RSH02, since validated by Smith, Henry, & Vishniac (2006, hereafter SHV06) of nonrepeating cycles in the light curve of γ Cas. These variations have a characteristic length of 60–90 days and have a full amplitude of $\simeq 3\%$. This amplitude increases slightly from the Johnson B to V filter bandpass. Interestingly, RSH02 also found that the X-ray flux of γ Cas varies by a factor of three over timescales of months. Moreover, these authors found that the X-ray and optical variations correlate very well with one another, a fact substantiated by more recent optical and X-ray observations reported by SHV06. Since they are both cyclical, they do not correlate with the star’s binary orbital phase.¹ The cyclical and “reddish” nature of the optical variations led RSH02 to propose that the X-ray variations in γ Cas are generated by a magnetic dynamo excited in the Be star’s (decretion) disk.

To see whether HD 110432 exhibits optical characteristics similar to the optical modulations that in γ Cas also correlate with X-ray variations, we undertook the photometric monitoring campaign described in §2.1. The results of our 2002 campaign in Sutherland showed an identical variability pattern in both V and B filter data. We exhibit our results for the V band in Figure 3a. This figure shows that after the start of the monitoring period the optical magnitude of HD 110432 faded rapidly by $3\text{--}3\frac{1}{2}\%$. After a gap in monitoring of nearly two months, the star once again regained its initial brightness. At the end of the observing season, the star’s faintness faded to its mean level. This variability is typical of a cyclical behavior in Be stars. If this particular cycle is representative of the variability of this star, then the cycle amplitude, waveform, and length are all similar to the optical cycles in γ Cas. In addition, according to the preponderance of scatter in the upper left of the constant-color relation of Fig. 3b, the star’s brightest changes were greater during these variations in the V band than the B band. These optical properties are similar to those RSH02 found for γ Cas.

5. Variability of the strong ultraviolet resonance lines

Codina et al. (1984) have discussed the strong wind absorptions in the blue wings of the resonance lines of CIV, NV, and SiIV at one epoch in 1981. This absorption is accentuated by the presence of DACs (Discrete Absorption Features) in the CIV and SiIV doublets. Figure 6 displays a sample of three *IUE* (*Short Wavelength Prime*) spectra in the

¹ γ Cas is a nearly circular binary with a period of 204 days, according to Harmanec et al. (2000) and Miroshnichenko, Bjorkman, & Krugov (2002). the mass and evolutionary status of the secondary of γ Cas are unknown. The binary status of HD 110432 is currently unknown.

neighborhood of the CIV doublet and SiIV line. These examples include the 1981 SWP spectrum discussed by Codina et al. (shown as the dotted line) as well as a mean of two spectra from 1986 and one spectrum from 1991. The 1986 and 1991 spectra indicate that the wind absorption in the CIV and SiIV (though not shown, also NV) doublets had been comparatively weak in 1981. In all epochs a rich array of DACs were present in the CIV lines, and indeed their detailed structure can be quite different. The wind absorption can be discerned in the CIV $\lambda 1548$ line out to -1800 km s^{-1} . Coincidentally or not, this is also the absorption edge limit found in resonance line spectra of γ Cas (e.g., Cranmer, Smith, & Robinson 2000, hereafter CSR00). Another similarity with the γ Cas spectrum is that the SiIV DAC typically has a single component located at about $-1100 \pm 200 \text{ km s}^{-1}$ (cf. Doazan et al. 1987, Smith, Robinson, & Corbet 1998).

In contrast to the very stable HeII $\lambda 1640$ discussed above, the resonance lines of SiIV, CIV, and even NV exhibit extensive variations even at low (positive and negative) velocities. The position line minimum can vary noticeably on a timescale of 2–3 days, suggesting that much of the central core is formed in the wind at some times. Moreover, as indicated by the dotted and dashed arrows in Fig. 6 the minima occurs at different velocities in the various ions at any given time. This leads us to wonder whether the feature, blueshifted to -100 km s^{-1} , and utilized by Codina et al. (1984) in the 1981 spectrum, gives a fair measure of the photospheric velocity field. A detailed check of the SiIV profiles during an intensive monitoring 2-day campaign in 1986 suggests that the central core and low velocities, out to -300 km s^{-1} , develop and stagnate at irregular intervals of several hours. For example, the absorptions in this region remain static for the spectra given by SWP 27967, 27970, and 27972, strengthen for SWP 27980, 27991, and 27997, and remain static again by the time of the SWP 28004 exposure. Similar patterns may be present, but less clearly in the blue wing of the leading member of the CIV and NV doublet. This type of activity is reminiscent of the recurrence of wind features on the timescale of many Be stars' rotational periods. In the particular case of γ Cas these patterns can be associated with particular regions close to the Be star's surface which in turn emit high X-ray fluxes and absorb UV continuum flux, respectively (Smith & Robinson, hereafter SR99; Cranmer, Smith, & Robinson 2000).

6. Optical high-resolution spectroscopy

6.1. Migrating subfeatures

6.1.1. *The migrating subfeatures in line profiles of γ Cas*

In 1988 Yang, Ninkov, & Walker discovered the existence of a peculiar new class of traveling bumps in the line profiles of γ Cas. These “migrating subfeatures” (*msf*) form in the blue wing and move at a rate exceeding the expected star’s surface rotation rate. They generally form in loose groups, and although they are usually present they can be occasionally absent on any given night. Often an *msf* can form or disappear (or both) during the time it moves across the line profile, and typically their lifetimes are 3 hours or less (Smith 1995). Although Yang, Ninkov, & Walker observed *msf* in the optical line profiles of γ Cas, these features have since been observed in high signal-to-noise time-serial ultraviolet spectra obtained by the Goddard High Resolution Spectrograph, formerly attached to the *Hubble Space Telescope* (SR99). Spectral line syntheses of the ultraviolet data suggests that the *msf* are likely the absorptions caused by intervening clouds anchored to the surface by putative magnetic fields (Smith, Robinson, & Hatzes 1998). In these higher quality data, it becomes apparent that faint *msf* are numerous and can be identified with lifetimes even as short as about 1 hour (SR99). Until this study, *msf* have been reliably reported in the line profiles of γ Cas and only one other star, AB Dor (Cameron Collier & Robinson 1989). The latter is an active, magnetic pre-main sequence K dwarf (e.g., Hussain et al. 2000). An additional discovery of *msf* was announced for the B5 star HR 1011 (Smith 1996), but adequate follow-up observations not yet been made. Additional authors have pointed to the existence of probably short-lived clumps of circumstellar gas close to Be stars (Smith & Polidan 1993, Smith 1995, Peters 1998, Zorec, Frémat, & Hubert 2001), which may be related to but do not technically qualify as *msf*.

6.1.2. *Discovery of migrating subfeatures in line profiles of HD 110432*

To investigate whether the line profiles of HD 110432 exhibit any type of rapid variability, we undertook the spectroscopic campaigns in 2005 January and February described above. From the resulting time sequences we computed greyscale from the difference spectra of each nightly mean spectrum. In these computations we first removed cosmic ray events and isolated bright pixels by correcting them to the mean flux of their neighbors. We also removed minor artificial continuum undulations from the initially computed difference spectra by removing undulations found in fifth degree polynomial fits.

In our grayscale results for six nights (the fifth of our seven nights in January was largely clouded out), we found clear *msf* patterns for two nights. These results are presented in Figure 8. This patterns were slightly weaker on the third night and weaker still on the fourth and sixth night. By the seventh night no *msf* pattern could be detected. Similarly, of three nights in February having 10 or more observations, *msf* were present on two of them and not on a third. Note on January 27th (see Fig. 8) the clear three narrow dark features running diagonally toward the upper right part of the grayscale. On January 25/26 one can see that the end of a first, and the beginning of a fourth, *msf*-like feature are present. In addition, we estimate an acceleration rate of $+100 \pm 10 \text{ km s}^{-1} \text{ hr}^{-1}$ in the *msf* features in Fig. 8. Within the errors this value is the same as the rate $+92 - 95 \text{ km s}^{-1} \text{ hr}^{-1}$ for the *msf* found in line profiles of γ Cas (e.g., Smith 1995, SR99).

The presence of small co-rotating clouds anchored to a rapidly rotating star seems to be a necessary condition for inferring the presence of magnetic fields in rapidly rotating stars. Clearly, this inference cannot be readily made from zeeman observations. For this reason any claim of detection of *msf* calls for a discussion of mechanisms that might confuse this interpretation. A reminiscent type of spectral pattern is the collection of traveling “bumps” produced on line profiles by high-degree nonradial pulsations (NRP). Although NRP are generally found in cooler spectral types than B1, they have been observed in late-O main sequence stars ζ Oph (e.g., Reid et al. 1993, Kambe 1997, Balona & Kambe, 1999, Walker et al. 2005) and HD 93521 (Howarth et al. 1998), and for the B0.5 IV-III star ϵ Per (Gies et al. 1999). The acceleration values of the migrating NRP bumps from NRPs in the line profiles of these massive stars cases tend to be clumped either at high values, e.g. near $150 \text{ km s}^{-1} \text{ hr}^{-1}$ for ζ Oph, and HD 93521, or at values much lower than the corotation rate, at $\approx 20 \text{ km s}^{-1} \text{ hr}^{-1}$ for ϵ Per.

Superficially, the line profile striations in these stars seem similar to the *msf* in line profiles of γ Cas. However, in general the dark striations caused by NRP and by intervening corotating clouds differ in several respects:

- i)* the spacings of *msf* are irregular, such that the time intervals between successive transits can change, while for monoperoiodic NRP the bumps are evenly spaced.
- ii)* the absorptions constituting the *msf* are confined to small wavelength intervals compared to the spaces between them. In contrast, the waveforms of monoperoiodic NRP are nearly sinusoidal. The dark and light bands in the grayscale depiction have nearly the same width.
- iii)* *msf* can be present on any one night and disappear or appear only sparsely on a second night. The available data suggest that both they and their associated X-ray activity centers have limited lifetimes of only one to a few days (Robinson & Smith 2000, RSH02). In

contrast, the NRP bumps are present every night, and their visibility varies over short timescales only because of the interference of bump systems arising from different modes of comparable strength.

iv) the *msf* in HD 110432 and γ Cas exhibit accelerations of 92–100 km s⁻¹ hr⁻¹. This is close to the value for rotational migration of a spot on the star’s surface, and yet also consistent with migrations from corotating clouds near the surface (e.g., Smith 1995, SR99). In the NRP paradigm an acceleration rate must be consistent with the intrinsic periods suggested by NRP theory. Such periods are thought to be of the order of the timescale in the metal bump zones in which they are driven (e.g., Pamyatynkh 1998), which are several hours for an early B-type main sequence star. In contrast, an acceleration rate consistent with surface corotation is by definition infinitely long in the corotating frame and therefore disallowed by NRP theory. From this argument, the observed acceleration rate in HD 110432 is consistent only with the corotation scenario.

v) *msf* seldom last during a full transit from the blue to the red wing whereas NRP bumps do so as a rule. High signal-to-noise observations of the UV lines of γ Cas (Smith, Robinson, & Corbet 1998, SR99) indicate that weak *msf* are ubiquitous in spectral regions with a dense packing of lines. While current optical spectra have permitted the identification of the stronger ones that last as long as 3 hours, higher quality *HST/GHRS* data shows that the more numerous faint ones exit with lifetimes even as short as about 1 hour (SR99).

vi) the acceleration of bumps produced by NRP in a line profile increases toward the edges of the line profile due to the foreshortening of the distance traversed by the waves toward the stellar line. A nice illustration of this effect is provided by Peters & Gies (2005) in their grayscale depicting NRP in π Aqr. In contrast, the *msf* enter/exit the profile edges with an acceleration closer to the value at the center of the profile. This is because the velocity vector of an elevated cloud has not completely rotated from a traverse to a radial orientation by the time the cloud has moved off the projected limb.

All of these *msf* attributes found for γ Cas are met in our observations of HD 110432. However, the first two points listed above are risky discriminators between NRP and corotating clouds in themselves. For NRP stars with multiple high-degree modes, like ζ Oph, the bands *can* sometimes appear at irregular intervals and appear as nonsinusoidal waveforms. Point *iii*, the occasional absence of features, is more difficult for NRP to mimic, although it could be reproduced if one sampled the line profiles at unlucky times. Even so, it is difficult for us to conceive that this coming and going of features could occur in the NRP interpretation both in our January and February monitorings.

Points *iv* and *v* constitute somewhat stronger arguments that these features are *msf*.

According to point *iv*, the observed acceleration rate in HD 110432 is consistent only with a corotation rate, presumably magnetically constrained, of a structure located near the star’s surface. In addition, the discovery of co-rotating clouds *close* to a star’s surface is preferred because of the rapid fall off ($1/r^3$) in magnetic field strength from the surface. The discovery of a star with an even larger magnetic field strength that could confine plasma at higher elevations would be correspondingly less probable.

Point *v* is likewise persuasive. From a perusal the data of Reid et al. (1993), the convenient observing timespan needed to differentiate between NRPs and *msf* on any particular night seems to be of the order of 7–8 hours. In this timescale, one can begin to decide whether the features are “permanent,” and that they do not disappear either because the intrinsic disturbance dissipates or because an elevated cloud responsible for it moves off the background stellar disk. Our observing durations are too short to provide this type of conclusive test. However, some of our features do disappear or appear suddenly near the middle of the profile, and this suggests short lifetimes.

Collier & Robinson (1989) have pointed out that the rotation of the velocity of a corotating cloud can be utilized to determine the cloud’s height around the star (point *vi*). In our data the limited signal-to-noise ratio and short lifetimes of the profile features limit our ability to make a good estimate. However, one can say that there is little evidence for a dramatic acceleration of the features near the $\pm v_r$ edges in our grayscale. This fact precludes the formation of these features on or within about $0.3R_*$ of the surface.

We conclude this discussion by stating that it is probable but not proven that the time-dependent striations we observe are induced by magnetically confined clouds. Clearly we cannot make firm conclusions in this regard based only on a few nights of data. The identification of *msf* properties in γ Cas itself was the result of several investigations of many UV and optical lines.

6.2. The optical emission spectrum

Because the instrumental configurations were static during our January and February observing runs, we could form average spectra from our two datasets. The coadded spectra for both epochs exhibited the same peculiarly shaped emission profiles noted by Slettebak (1982). The only prominent absorption lines in our spectra are the first three Balmer lines and the helium HeI 4471 Å, 5876 Å, and 6678 Å lines. Of these features, only $\lambda 4471$ is present entirely in absorption. Other light-element lines have absorption wings and the same double-lobed emission cores as the metallic lines. We will discuss the absorption features

further in §6.3.

6.2.1. Identification and profiles of emission features

HD 110432 has an optical spectrum contains numerous permitted hydrogen, helium, and metallic lines in emission. For this reason already it belongs to a subset of “classical Be stars”² with this characteristic. Also, the profiles are marked by a flat central emission plateau flanked by stronger V and R lobes. This type of double-peaked emission profile is common in a small subset of classical Be stars and has been modeled by Hanuschik (1988) and Hanuschik et al. (1996). The double-lobed profile is a signature of an optically thin Keplerian disk with little or no radial expansion or contraction. The star-disk system is seen nearly edge-on (precisely edge-on systems show a narrow central “shell” component not present in our spectra of HD 110432). Moreover, the two peaks are generally slightly unequal. Over time they track the famous V/R cyclical variations of Balmer line profiles over years. Examples of Be stars that have about the velocity separation for the two peaks, according to these authors, are α Col, 25 Ori, HR 2787, ω Ori, and HR 2284.

We began our analysis by determining the wavelengths of the emission features in the January coaddition spectrum. After correcting for the star’s radial velocity of $+9 \text{ km s}^{-1}$, determined by TTW73, we measured the centroid velocities of the features. We found a mean radial velocity of $+6 \pm 5 \text{ km s}^{-1}$ for the emission features we could reliably measure. This value agrees well with our adopted velocity for the star.

Next, we identified lines by computing synthesized LTE spectra using the *SYNSPEC* and *CIRCUS* codes. We utilized *CIRCUS* to simulate the effects of a putative circumstellar “cloud” located outside the direct line of sight to the star. The contribution it makes to emission can be computed for any arbitrary doppler velocity. We performed trial computations for models with several temperatures and obtained a good match with the line opacity spectrum computed with $T = 10,000 \text{ K}$. The identifications, the excitations of the lower atomic levels, and measured and computed equivalent widths of the V and R emission lobes are indicated in Table 1. Almost all the lines in the spectrum are Fe II lines. Typically these have excitations of a few eV, as noted in the table. Equivalent widths are not given in the table for those cases for which line strengths are too weak to make a reliable measurement, or for which two or more pairs of V , R lobes are present because of contributions from neighboring lines. The He I lines are listed twice, once for the January and February observing

²The spectra of classical Be stars have Balmer emission lines produced by decretion disks. These disks are formed neither by protostellar collapse or binary mass transfer.

runs. A comparison of these entries demonstrates that He I line strengths increased during this interval.

Figure 9 shows a montage of profiles of the He I 5876 Å and 6678 Å lines, as well as a selected group of metallic Fe II lines for both January and February spectra.³ In aligning the spectra in our figure, we corrected for the star’s radial velocity. The vertical lines in the figure denote the centroid negative and positive velocities of the *V* and *R* peaks.

A comparison of the shapes of the emission lines in Fig. 9 reveals that they are virtually identical for lines of any ion. However, small differences in *strengths* are evident from epoch to epoch. First, the February profiles show peaks that are closer together than the January profiles ($\pm 115 \text{ km s}^{-1}$, instead of $\pm 102 \text{ km s}^{-1}$). Second, the February metallic-line emissions represent a $\sim 10\%$ strengthening over the previous month. An additional property of the red He I lines in both datasets is that the ratio of $\lambda 5876$ to $\lambda 6678$ emission equivalent widths is close to 2. Because the ratio of the atomic *gf* values for these two lines is 2.5, this value indicates that the He I lines are nearly optically thin. However, the decrease of the ratio in our February data, along with a small strengthening of the Fe II lines, could indicate some increase in the column density of the disk during this period. According to our simulations below, the metallic lines are optically thin ($\tau \leq 0.1$).

6.2.2. Analysis of the emission spectrum

The double-lobed structure we observe in the optical spectrum of HD 110432 is the classical shape of an optically thin disk viewed nearly edge-on. Therefore, we have assumed that this is the correct viewing geometry in evaluating the equivalent widths of these lobes. We measured equivalent widths by assuming that the lobes have gaussian cores and symmetric extended wings. We measured their half equivalent widths by measuring their contributions between wavelengths defining the central core of the lobe and the point where the wing merged with the stellar continuum, typically 50 km s^{-1} from the centroid of the core. In column 4 of Table 1 we list the sums of these values for the *V* and *R* lobes. These are the means of the equivalent widths of these two features. The last column of the table is the computed equivalent width obtained from the $T = 9,800 \text{ K}$ model defined below. This value is computed by subtracting the narrow contribution of the disk component produced by *CIRCUS* from the rotationally broadened photospheric line given by *SYNSPEC*. Since the

³We can add from an examination of a few archival spectra obtained with the ESO 3.6-m. Coude Echelle Spectrograph, that certain weak lines (e.g., Fe II 4309 Å) have emission profiles similar to those in our montage.

observed profiles in Fig. 9 are the same *inter alia*, to within our errors of measurement, we can evaluate attributes such as the strengths of their emission lobes straightforwardly.

The determination of specific parameters for our homogenous disk model proceeded according to the following steps:

a) Disk Temperature Lines of neutral helium and Fe^{1+} co-exist in the optically thin regime only in a narrow region of temperature. Therefore, we have exploited this fact to use the ratio of the strengths of these lines to determine T_{disk} . Using *CIRCUS* models, we found that the number of helium atoms populating their 21 eV levels drops quickly from a moderate finite value at 11,000 K to effectively zero at 9,300 K ($N_e = 10^{11} \text{ cm}^{-3}$), assuming normal chemical abundances. The single temperature that best fits the observed ratios in Table 1 is $9,800 \pm 200 \text{ K}$. The error bars on this figure are determined as much by our lack of precise knowledge of the volumetric electron density as by photometric or measurement errors.⁴

b) Column density: The measured equivalent width ratio of the helium lines $\text{EW}(\lambda 5876)/\text{EW}(\lambda 6678) \approx 2.0$ provides a rough estimate of the optical depth in these lines. Having estimated the disk temperature from item *a*, we computed models with varying mean column densities until we found a value that produced a match with this equivalent width ratio. We found the most probable value is $3^{+2}_{-1} \times 10^{22} \text{ cm}^{-2}$. The errors here are based on the temperature errors given above, combined with an assumed $\pm 5\%$ error in the measured equivalent width ratio. Note in this region of temperature-depth space, the propagation of the errors is asymmetric around the mean value. For this column density, temperature, and microturbulence (see *c*) the Fe II $\lambda 5018$ and $\lambda 4923$ lines are marginally optically thick, having $\tau_{\text{line}} = 2$ and 1, respectively. The optical thickness of the strongest helium line, $\lambda 5876$, is 0.2.

c) Microturbulence: This value was determined by matching the ratios of Fe II lines having the same excitations but comparatively low and high *gf* values, e.g. $\lambda 4923$ and $\lambda 5018$. The value determined from these ratios in our line syntheses is $\xi = 10 \pm 3 \text{ km s}^{-1}$.

d) Projected area: Finally, the strength of absorption or emission lines sets the projected star disk in natural units of a star area, πR_*^2 . Note that all other quantities outlined in *a-c* utilize line strength *ratios*. The projected area we determine from our *CIRCUS* models is the value used to match the *absolute* computed strengths to the observed ones (columns 4 and 5 in Table 1). The computed area is $100 \pm 10 R_*^2$ (the error bars are internal). Since the disk is almost in the thin regime, and we may reasonably expect it to be at least roughly axisymmetric, considerable degeneracy exists for estimates of disk area and the column density. While the density in particular is not well determined, the volume estimate is more

⁴We believe that the poor fit for the Fe II 6318 Å may be due to inaccurate atomic data for this line.

secure. Assuming a stellar radius of $7R_{\odot}$, the equivalent disk volume and mass for the homogeneous model parameters are $\sim 10^{48} \text{ cm}^3$ and $\sim 10^{-9} M_{\odot}$. This is a typical mass for a well-developed disk of a classical Be star disk.

As a clarification, we should note that the solution described above represents a volume-weighted mean for the sector of the assumed homogeneous disk we have considered. A more realistic approach to modeling the disk segment in the sky plane might take into account that the disk temperature and hence the He I/Fe II emission should vary with distance from the star. To evaluate the effects of a temperature gradient, we fit several lines in Table 1 with a *two-temperature* component solution, that is with two distinct but equal volumes having the same column densities and arbitrarily chosen temperatures of 10,000 K and 9,000 K. (Because the radius-temperature relation is unknown, distances of these two disk components along the line of sight are unknown.) We also scaled the areas of the two equal-area components until they fit the He I and Fe II lines in the table to the same precision as our first model. We found a good match when the two subareas were 37 stellar areas each. This is not to say that the two-parameter model is a better fit to the equivalent width data than our single parameter model given above. Rather, it demonstrates only that the added sophistication reduces the area by only 26%. We can conclude that the large areas in our solutions do not seem to be strongly determined by radial temperature gradients through the disk.

A second important point to come out of our analysis relies on the kinematical argument already alluded to in our reference to the work by Hanuschik (1988). In the case of HD 110432110, the velocity separation of the *V* and *R* lobes is Keplerian, the region where they are formed is roughly 1.06 A.U., assuming a stellar mass of $12 M_{\odot}$. This leads us to evaluate whether the temperature we have derived, 9,800 K, is reasonable for the disk of a B1e star. By way of comparison, we take consider the theoretical analysis of this star’s disk by Millar & Marlborough (1998). In their analysis of the radiative energy losses and gains, these authors found a density-weighted mean temperature of 10,800 K. This determination is in reasonable agreement with the value of $9,500 \pm 1000 \text{ K}$ that Hony et al. (2000) derived in their analysis of the bound-free absorption edge of the hydrogenic Humphreys jump in infrared spectra. However, according to these authors this emission is formed primarily within a few stellar radii from the surface of $\gamma \text{ Cas}$. Millar & Marlborough’s results indicate that the disk temperature decreases slowly with stellar distance. Thus, an extrapolation of their model out to $\approx 1 \text{ A.U.}$ ($\sim 30R_{*}$) would certainly predict a lower value than we have found, even though $\gamma \text{ Cas}$ is likely to be the hotter of the two stars. In this event, it may be that nonradiative heating is required to maintain the temperature of the HD 110432 disk.

Third, we note that our disk dimensions, especially an extension out of the plane, do not necessarily agree with those of other well studied stellar disk systems. In particular, Be disks

originating from decretion or protostellar collapse have densities that are strongly confined to the equatorial plane, and their contours flare outward from the plane. The well studied disk of γ Cas is a case in point. As mentioned above, observations show that a typical electron density at a typical point of this disk is $\sim 10^{12} \text{ cm}^{-3}$, and the column density in the poloidal direction is about 10^{23} cm^{-2} (Millar & Marlborough 1998). Interferometric observations in $\text{H}\alpha$ light find that hydrogen is ionized out to a radius of about $6R_*$ (Quirrenbach et al. 1997). A comparison with this detailed description does not allow much leeway to extend the disk of HD 110432 in the radial direction. Given the optical thinness of all the lines, including of He I, the only effective way to realize a large projected area is to invoke a geometry in which the disk flares outward from the plane by several R_* . We trust that this apparent peculiarity will turn out to be a clue to resolving how this star’s disk is maintained.

As a fourth consideration, the question arises whether similar emission features might also be present in the γ Cas spectrum. In fact, Bohlin (1970), Slettebak (1982), and evidently TTW73 have already noted Fe II emission lines, including the first two Fe II entries in our table, and unidentified “chromospheric” lines, some of which overlap those in Table 1, were identified long ago by Heger (1922). Bohlin’s paper also referenced the identification of iron emission lines by Baldwin (1942) and Cowley & Marlborough (1968) using moderate-dispersion photographic plates. In the intervening time, it appears that neither the strengths nor the shapes of these features have been studied in the γ Cas spectrum. However, from our analysis of the HD 110432 optical spectrum, we can predict that future observations of the γ Cas spectrum will disclose numerous emission lines with plateau-shaped profiles. Because γ Cas presents an intermediate observing angle, it is not clear that its emission line profiles will include a well-resolved lobe structure, although this may still turn out to be the case. In any case, the fact that the lines are present in the γ Cas spectrum confirms our geometrical picture that the lobe-structure in the HD 110432 spectrum is due to Keplerian rotation of the disk.

6.3. The absorption lines of HD 110432

6.3.1. Description

The only optical line entirely in absorption in our spectra is He I 4471 Å. In Be stars the nearby Mg II 4481 Å line is generally easily identifiable, despite its position in the red wing of the He I feature. In our spectrum the Mg II feature has been overwhelmed by the particularly strong absorption red wing of He I. The wings of this line are broadened symmetrically to $\approx \pm 1000 \text{ km s}^{-1}$. This smearing is shown for the He I $\lambda 4471$, $\lambda 5876$, and $\lambda 6678$ lines in Fig. 7. This same characteristic is shared by first three Balmer members.

This broadening is unlikely to be instrumentally induced for at least two reasons. First, the spectrograph has been used for years to observe spectra of other rapidly rotating AB stars, and the recovered profiles are normal and are in agreement with other instruments. For example, Balona & James (2002) have studied the line profiles of several of the HeI and Balmer lines in question, including $\lambda 4471$. The wings and associated nearby continua exhibit no abnormalities. Likewise the profiles in our January and February spectra show no systematic differences from one another. Second, we may assess the reliability of the continuum and echelle blaze functions by comparing the echelle order ($m = 45$) containing the $\lambda 4471$ line with the instrumental continua of the two neighboring echelle orders. In Fig. 7 this spectrum, and implicitly the associated internal errors, are labeled by the annotation “Continuum.” The key point of this comparison is that fluxes of the auxiliary spectra show no, or at most a minor deviation, from flatness across the central region of the blazes.

We have also considered spectra of other objects taken during the January and February runs with the same instrumental configuration. In Fig. 7 we also exhibit the spectrum of the order containing $\lambda 4471$ for the roAp star HR1234 observed during the January run. We note that an A3 star was observed during the February run. Once again, the orders containing this line and the red helium lines were flat whereas the spectra of HD 110432, reduced in exactly the same way, showed the characteristic $\pm 1000 \text{ km s}^{-1}$ broadening.

It is important to note that the core depth $\lambda 4471$ in our spectra is 10%. According to profiles of the same line in the spectra of γ Cas (Chauville et al. 2001) and other rapidly rotating B0-2V stars found in the UVES Paranal spectral atlas (Bagnulo et al. 2003), this is the nominal depth of this line in spectra of rapidly rotating early-type Be stars. Rotational broadening dominates the shape of the (weak) far wings in the latter cases, a fact we have confirmed in our own spectral syntheses of hydrogen and helium lines. For this reason the absorption lines should be characterized as *strengthened* as well as anomalously broadened.

The only other published report of an optical-wavelength helium line profile is that of Ballereau, Chauville, & Zorec (1995) atlas of $\lambda 4471$, $\lambda 4481$, and $H\gamma$ profiles of Be stars. The $\lambda 4471$ of HD 110432 in this atlas is somewhat peculiar, exhibiting both a sharp line core and triangular wings, and in this sense it appears unlike other $\lambda 4471$ profiles in the atlas. Nonetheless, it is quite unlike the profile in 2005. It is evident that the line’s shape, if not strength, has changed on a timescale of several years.

6.3.2. *The unknown broadening agent*

In any context the presence of the strong absorption lines broadened by more than twice the star’s likely rotational velocity presents an interpretational challenge. These absorption lines cannot arise from the blended superposition of two components of a double-lined binary because this circumstance would not produce the substantially strengthened lines we observe. Moreover, spectra of a presumed near edge-on Be-binary system should exhibit radial velocity variations within a few days, and these have not been observed. In this model, lines might be rendered broad and unresolved at certain phases, but they would not be strengthened.

Because the star’s parallax is in agreement with its spectroscopic luminosity class, it is hardly possible for a compact star such as a white dwarf to dominate the flux contribution of the B star and produce Stark broadened wings. However, the profiles in Figs. 7 and 9, including $H\gamma$ and the companion profiles of the February dataset (not shown) indicate that the line wings end abruptly at a flat continuum some $1100\text{--}1300\text{ km s}^{-1}$ from line center. In this sense they do not resemble the gradual merging into the continuum of pressure-broadened line profiles.

At the referee’s suggestion (and for the moment suspending our knowledge that HD 110432 occupies a position in the H-R Diagram appropriate to a $\sim B1\text{ IV}$ star and also that the profiles seem to be variable over an underdetermined long timescale), we have also investigated the line profiles of the He I lines in the early DB white dwarfs. In surveying the literature, we find it is comparatively easy to find examples of 4471 \AA profiles that are Stark broadened to considerable degrees (Wesemael et al. 1993, Liebert et al. 2003). However, many of these same spectra exhibit no visible He I red lines. The red lines of two sdB stars observed by Heber & Edelmann (2004) exhibit very weak wings. Among three early DB stars observed by Wolff et al. (2002), only one of them has spectral line wings that extend to $\pm 350\text{ km s}^{-1}$. We can conclude that since the Stark components are weak in the red lines of these sdB and DB stars, the excess broadening found in the helium and hydrogen lines of our spectra obtained in 2005 is not caused by pressure broadening. This conclusion is likely to extend to the other broadened lines in the blue spectral region.

Electron scattering can also broaden lines over a velocity range characteristic of the temperature in a hot gas. However, this mechanism is conservative in the sense of redistributing monochromatic flux rather than a strengthening of a line. Moreover, for electron scattering to be effective the required very high column densities ($10^{24\text{--}25}\text{ cm}^{-2}$) are not present near HD 110432, according to both analyses of our optical emission line spectrum and of the gradient of the X-ray continuum (TO01).

By process of elimination, we are left with invoking doppler velocities to explain the

excess absorption line widths in optical lines. However, we have no information at the moment to link such velocities to other phenomena, including the X-ray emissions. We will continue to monitor this star’s optical spectrum both to confirm this behavior and to investigate whether the broadening evolves in the coming years.

7. Conclusions

HD 110432 is an unusual Be star, whether studied in the X-ray, ultraviolet, or visual regimes. Its hard X-ray spectrum is probably thermal (TO01). As shown in Figs. 5 and 4, its optical light curve for the year 2002 shows modulations which arguably are similar to those observed in γ Cas. This makes HD 110432 a fascinating target because it makes its association with the highly enigmatic γ Cas possible. Although the far-UV and UV lines are representative of a rapidly rotating B1 star, like a number of Be stars its resonance lines show variations on a timescale of a few days, or perhaps much less. The hydrogen and helium line absorptions of the *Giraffe* spectra obtained in January and February 2005 appear to be “almost photospheric.” These lines suggests a \approx B1 spectral type that is consistent with the spectral energy distribution determined by Codina et al. (1984). However, the wings of these lines are strengthened by a broadening corresponding to $\approx\pm 1000$ km s $^{-1}$. The cause of this broadening is unknown.

A number of metallic emission lines chiefly due to Fe II are present in the green-red spectrum. These features exhibit a central plateau flanked by two *V* and *R* emission peaks. This same profile is shared as an inner core feature of the first three members of the hydrogen Balmer series and the He I $\lambda 5876$ and $\lambda 6678$ lines. The *V* and *R* peaks of all these emission lines are separated by about 200 km s $^{-1}$. Both the separation velocity and the strengths of the features can vary on a timescale of a month. We can conclude from *i*) the shape of the emission line profiles, *ii*) the equivalent width ratio of the features in the two “red” He I lines, and *iii*) analogous emissions in the γ Cas spectrum that the emission lobes are formed in an optically thin, Keplerian disk extending out to about 1 A.U. from the star. Using this basic geometry, we can solve for the parameters of a homogeneous disk. Along the sight line of maximum elongation of the projected disk, the mean disk temperature is close to 9,800 K, the column density through this region of the disk is roughly 3×10^{22} cm $^{-2}$, and the projected area is some 100 stellar areas. (A likely small decrease in the He I line ratio could indicate a mean column density of perhaps 4×10^{22} cm $^{-2}$ at this epoch.) The latter value is quite large and suggests that the disk flares from the central disk plane. The computed disk area can be reduced by assuming that the disk has an arbitrary temperature gradient. At a distance of ≈ 1 A.U. from the star, a gas temperature of 9800 K may be difficult to maintain from

the star’s radiative flux alone. Therefore, it is possible that an additional heating source is required.

The X-ray and optical properties of HD 110432 are similar to those of γ Cas, a fact that suggests that the production mechanism of the X-rays may well be the same for these two stars. They are both early-type stars near the main sequence with a high rotation rate, even for a Be star. Their disks are well developed and both exhibit metallic and emission line spectra. In assessing the X-ray properties, we see that both stars exhibit signatures of plasma with a temperature of about 10^8 K and variations over a timescale of hours that can be characterized, at least with the available light curve, as chaotic meandering. We might hazard a prediction that, as with γ Cas, future high quality X-ray light curves of HD 110432 will show nearly continuous flaring and (from interaction with an extensive disk), and a visible fluorescent Fe K line at 6.4 keV. Turning to our own optical work, first in a ground-based photometric campaign in 2002, the star’s light curve during this season undergoes modulations with an amplitude of at least 3% that are consistent with a cyclical variation of about 130 days. This is consistent with the optical cycles of γ Cas, which have cycle lengths of about the same amplitude of 2–3 months. In both stars the cycle amplitudes increase from the *B* to *V* filter wavelengths. From an analysis of a spectroscopic time series of the red He I lines over several nights in early 2005, we have also found traveling absorption features migrating through the profiles at a rate equal to the *moving subfeatures* often visible in the profiles of γ Cas. Such features are highly unusual in Be stars, and indeed so far are clearly present only in γ Cas itself. Their existence is best, though not uniquely, explained by absorptions of small clouds that are locked into co-rotation by surface magnetic fields. This explanation has been bolstered by the recent report of the discovery of a long-lived periodicity of 1.21 day on γ Cas, probably caused by rotational modulation of a magnetic surface structure (SHV06).

From these observations we suggest that HD 110432 is the first new member of what may be called a “ γ Cas class” of X-ray Be stars, so far consisting of two stars. In the case of γ Cas, the prevailing evidence is that these X-rays are produced in the immediate vicinity of the Be star itself, perhaps by magnetic disk-star interactions (RSH02). Whatever the physical site, we may begin to evaluate candidate X-ray production mechanisms by examining the properties of both the X-ray and the star among members of this new class. Moreover, the greater the number of stars amassed in this class, the greater will be the probability of monitoring disk changes as they occur, and thus of determining the relevance of the disk to the high X-ray emission. We note a paper by Motch et al. (2006) that came to our attention as this paper was being completed has identified five possible γ Cas analogs, including HD 110432 as the brightest, based on their X-ray and optical properties.

In assessing differences in phenomenology that might be observed in γ Cas and HD 110432, the aspect angle to the observer could play an important role. According to interferometric studies of γ Cas (e.g., Quirrenbach et al. 1997), the star-disk system is observed from an intermediate obliquity. Smith et al. (2004) found that its *Chandra* continuum spectrum is attenuated at longer wavelengths in such a way as to require a two column-density absorption model to fit it. If the X-rays arise from a star-disk interaction, this model fits in well with the expectation that these emission would be emitted from two types of sites, one primarily in front of the disk along the line of sight and the other behind it. If one were to observe γ Cas or an equivalent Be star from an edge-on orientation, and further, were to assume that most of the emission occurs outside the disk plane, then one might expect the continuum to be fit to a single column-density model. The column length derived would be high if the active centers were close to the disk plane but nearly zero if they were distributed far from the plane. The line spectrum of H-like light ions and Fe L-shell ions are primarily located between $\approx 8\text{--}17\text{\AA}$ more or less intermediate between the wavelength ranges used in the continuum to derive column absorption properties. A change in observer aspect should leave the line spectrum in this intermediate wavelength range less changed. Interestingly, T001 found an intermediate column density of 10^{22} cm^{-2} . A high-resolution spectrum should be able to address this question further and lead to constraints on the geometry of the formation region. Proceeding in the opposite direction, an understanding of disk dynamos could lead to an understanding of conditions in the inner disk.

This paper could not have been written without help from a number of colleagues who provided us with information and encouragement to unravel peculiar properties of this star. Thanks are due first to Dr. J. Torrejón and the editor of the *Astronomy & Astrophysics* journal for giving their permission to utilize the light curve figure from the T001 paper. We also acknowledge a number of helpful discussions about the properties of this star by Drs. Alex Fullerton, Steve Howell, Ted Snow, and Janez Zorec. We also thank Drs. Andrea Torres and Adela Ringuet for providing us with unpublished diagrams of the dependence of the He II $\lambda 1640$ line on rotation. We gratefully acknowledge the fruitful efforts of Mr. Francois van Wyk, who carried out the photometric monitoring on HD 110432 in 2002 and of Dr. David Laney who kindly obtained many spectra of this star during 2005 February. The quality of this paper was significantly enhanced from comments by an anonymous referee.

REFERENCES

- Bagnulo, S., Cabanac, R., Jehin, E., Ledoux, C., & Melo, C. 2003, “The UVES Paranal Observatory Project,” http://www.sc.eso.org/santiago/uvespop/field_stars_uptonow.html
- Baldwin, R. B. 1942, *Sky & Telescope*, 1, No. 9, 5
- Ballereau, D., Chauville, J., & Zorec, J. 1995, *A. & A. S.*, 111, 423
- Balona, L. A., & James, D. J. 2002, *MNRAS*, 332, 714
- Balona, L. A., & Kambe, E. 1999, *MNRAS*, 308, 1117
- Baudrand, B., & Bohm, T. 1992, *A. & A.*, 259, 711
- Bohlin, R. C. 1970, *ApJ*, 162, 571
- Cameron Collier, A., & Robinson, R. D. 1989, *MNRAS*, 236, 57
- Chauville, J., Zorec, J., et al. 2001, *A. & A.*, 378, 861
- Codina, S. J., de Freitas Pacheco, J. A., Lopes, D. F., & Gilra, D. 1984, *A. & A.*, 57, 239
- Cowley, A. P., & Marlborough, J. M. 1968, *PASP*, 80, 42
- Cranmer, S. R., Smith, M. A., & Robinson, R. D. 2000, *ApJ*, 537, 433
- Doazan, V., Bourdonneau, B., et al. 1987, *A. & A.*, 182, L25
- Feinstein, A., & Marraco, H. G. 1979, *AJ*, 84, 1713
- Gies, D. R., Kambe, E., et al. 1999, *ApJ*, 525, 420
- Hanuschik, R. W. 1988, *A. & A.*, 190, 187
- Hanuschik, R. W., Hummel, W., et al. 1997, *A. & A.S.*, 116, 309
- Harmanec, P., Habuda, P., et al. 2000, *A. & A.*, 364, L85
- Heber, U., & Edelmann, H. 2004, *Astrophys. & Sp. Sci.*, 291, 341
- Heger, M. L. 1922, *Lick Obs. Bull.*, 108, 1921
- Hiltner, W. A., Garrison, R. F., & Schild, R. E. 1969, *ApJ*, 157, 313
- Hony, S., Waters, L. B., et al. 2000, *A. & A.*, 355, 187
- Houk, N., & Cowley, A. P. 1975, *University of Michigan Catalog of Two Dimensional Spectral Types for the HD Stars*, Ann Arbor: Univ. of Michigan
- Howarth, I. D., Townsend, R. H. D., et al. 1998, *MNRAS*, 296, 949
- Hubeny, I. 1996. & Heap, S. R. 1996, *ApJ*, 470, 1144
- Hubeny, I., Lanz, T., & Jeffery, S. 1994, *Newslett. Anal. Astron. Spectra*, 20, 30

- Hussain, G. A., Donati, J. F., Collier Cameron, A., & Barnes, J. R. 2000, *M.N.R.A.S.*, 318, 961
- Kambe, E., Hirata, R., et al. 1997, *ApJ*, 481, 406
- Kurucz, R. L. 1990, *Trans. IAU*, 20B, 169 and <http://kurucz.harvard.edu/atoms/AEL>
- Kurucz, R. L. 1993, *ATLAS9 Stellar Atmospheres and 2 km s⁻¹ Grids*, Kurucz CD-ROM #13
- Liebert, J., Harris, H. C., et al. 2003, *AJ*, 126, 2521
- Marlborough, J. M., & Cowley, A. P. 1968, *PASP*, 80, 42
- Meyer, D. M., & Savage, B. D. 1981, *ApJ*, 248, 545
- Millar, C., & Marlborough, J. M. 1998, *ApJ*, 494, 715
- Miroshnichenko, A. S., Bjorkman, K. S., & Krugov, V. D., 2002, *PASP*, 114, 1226
- Motch, C., Lopes de Oliveira, R., et al. 2006, in *Active OB Stars: Laboratories for Stellar & Circumstellar Physics*, ed. S. Stefl, S. Owocki, & A. Okazaki, (San Francisco: ASP), in press
- Owens, A., Oosterbrock, T., Parmar, A., Schulz, R., Stöwe, J., & Haberl, F. 1999, *A. & A.*, 348, 170
- Pamyatnykh, A. 1998, in *ASP Conf. Ser. 135, A Half Century of Stellar Pulsation Interpretation. A Tribute to Arthur N. Cox.*, ed. P. A. Bradley & J. A. Guzik, (San Francisco: ASP), 135, 268
- Perryman, M. 1997, *The Hipparcos and Tycho Catalogues*, ESA SP-1200 (Noordwijk: ESA)
- Peters, G. P. 1998, *ApJ*, 502, L59.
- Quirrenbach, A., Bjorkman, K., et al. 1997, *ApJ*, 479, 477
- Rachford, B. L., Snow, T. P., et al. 2001, *ApJ*, 555, 839
- Reid, A. H., Bolton, C. T., et al. 1993, *ApJ*, 417, 320
- Robinson, R. D. & Smith, M. A. 2000, *ApJ*, 540, 474
- Robinson, R. D. & Smith, M. A., & Henry, G. W. 2002, *ApJ*, 575, 435
- Slettebak, A. 1982, *ApJS*, 50, 55
- Smith, M. A. 1995, *ApJ*, 442, 812
- Smith, M. A. 1996, *ApJ*, 469, 336
- Smith, M. A., Cohen, D. H., et al. 2004, *ApJ*, 600, 972
- Smith, M. A., Henry, G. W., & Vishniac, E. 2006, *ApJ*, submitted

- Smith, M. A., & Polidan, R. S. 1993, *ApJ*, 408, 323
- Smith, M. A., & Robinson, R. D. 1999, *ApJ*, 517, 866
- Smith, M. A., & Robinson, R. D. 2003, in *ASP Conf Ser.* 292, *Interplay between Periodic, Cyclic, and Stochastic Variability*, ed. C. Sterken (San Francisco: ASP), 263
- Smith, M. A., Robinson, R. D., & Corbet, R. H. D. 1998, *ApJ*, 503, 877
- Smith, M. A., Robinson, R. D., & A. P. Hatzes 1998, *ApJ*, 507, 945
- Thackeray, A. D., Tritton, S. B., & Walker, E. N. 1973, *Mem. Royal Astron. Soc*, 77, 199
- Torrejón, J. M., & Orr, A. 2001, *A. & A.*, 377, 148
- Walker, G. A. , Kuschnig, R., et al. 2005, *ApJ*, 623, L145
- Wolff, B., Koester, D., et al. 2002, *A. & A.*, 388, 320
- Yang, S., Ninkov, Z., & Walker, G. A. 1988, *PASP*, 100, 233
- Wesemael, F., Greenstein, J. L., et al. 1993, *ApJ*, *PASP*, 105, 761
- Zorec, J., priv. comm. 2005
- Zorec, J., Ballereau, D., & Chauville, 2000, in *ASP Conf. Ser.* 214, *The Be Phenomenon in B Stars*, ed. M. Smith, H. Heinrichs, & J. Fabregat, (San Francisco: ASP), 502
- Zorec, J., Frémat, Y., & Cidale, L. 2005, *A. & A.*, 441, 235
- Zorec, J., Frémat, Y., & Hubert, A. M., 2000, in *ASP Conf Ser.* 214, *The Be Phenomenon in Early-Type Stars*, ed. M. Smith, H. Heinrichs, & J. Fabregat, 330

Figure Captions

Fig. 1.— A FUSE spectrum of HD 110432 and a spectrum of γ Cas shown (dashed line) for reference for the wavelength region $\lambda\lambda 1115\text{--}40$. The light solid line is a scaled synthetic spectrum of the photosphere modified by a minor contribution from a warm circumstellar disk. The synthetic spectrum has been broadened by a rotational quasi-convolution of 300 km s^{-1} .

Fig. 2.— A comparison of spectra in the wavelength region surrounding the He II $\lambda 1640$ line of HD 110432 (all available 13 IUE/SWP spectra), γ Cas (all 31 small-aperture IUE/SWP spectra obtained in 1982), and the SYNSPEC-synthesized spectrum.

Fig. 3.— Panel *a* shows the Cousins V-band light curve of HD 110432 during 2002 February–June. If this variation is a cycle, it has a length of perhaps 130 days. Panel *b* shows a scatter diagram of the V- and B-band variations for the monitoring shown in panel *a*. The reference for the points in the upper left of panel *b* indicates that the optical variations are slightly larger for the V-band than the B-band.

Fig. 4.— A *RXTE* light curve of γ Cas from a 6-hour section of the *RXTE* light curve obtained on 1998 November 25–26; the solid line is the sine curve from Fig. 5. Its amplitude and period are the same as in the first case. Only the mean flux level of this curve has been modified to fit the γ Cas flux.

Fig. 5.— A 5-hour *BeppoSax* light curve of HD 110432 constructed by Torrejon & Orr (2001). The solid curve is a 4-hour sine wave fit to the dip in the middle of the observations. *By permission of Astronomy & Astrophysics.*

Fig. 6.— Sample observations of the CIV doublet complex (bottom) and SiIV $\lambda 1403$ (top) for epochs in 1981, 1986, and 1991, respectively; the abscissa is velocity. The rest positions of the CIV doublet are indicated by the λ_o symbols. The IUE/SWP observing sequence numbers are indicated. Dashed and dotted arrows indicate the positions of the central minima discussed in the text.

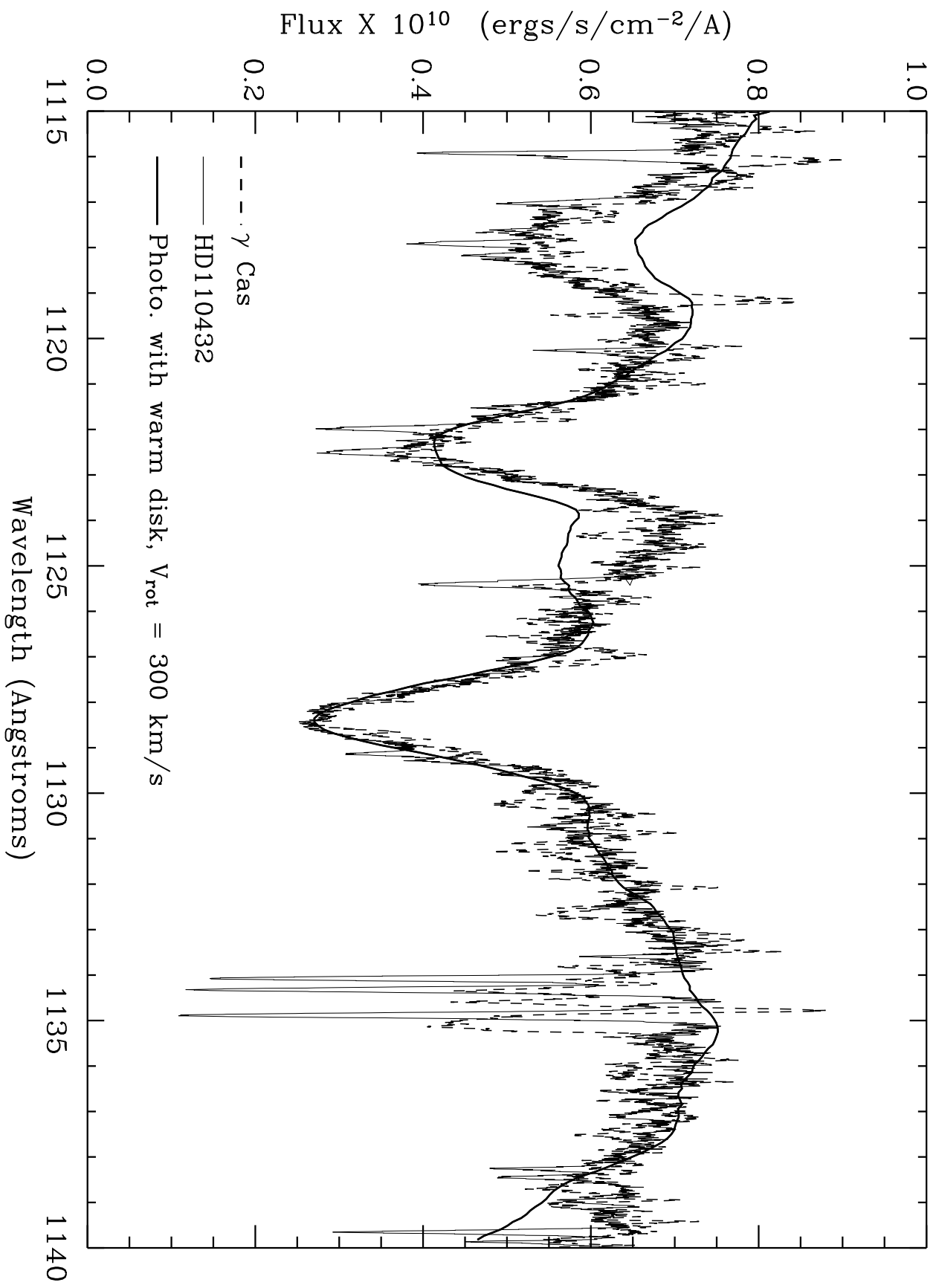
Fig. 7.— A comparison of three highly broadened neutral helium lines from our January 2005 SAAO *Giraffe* observations, offset for clarity. Vertical dotted lines indicate the approximate velocity limits of the wings of the lines. The nearly “Continuum” lines at the bottom are the superimposed spectra of the two neighboring echelle orders from the same observations. Note that the red wing of the $\lambda 5876$ spectrum has been truncated by the edge of the blaze. The spike at the red edge of the $\lambda 6678$ spectrum (scaled by a factor of two) is a grating-induced Wood’s anomaly. The plot at the bottom is the spectrum of the wavelength region near $\lambda 4471$ of the roAp star HR 1234. This spectrum was obtained during the January run when HD 110432 was observed.

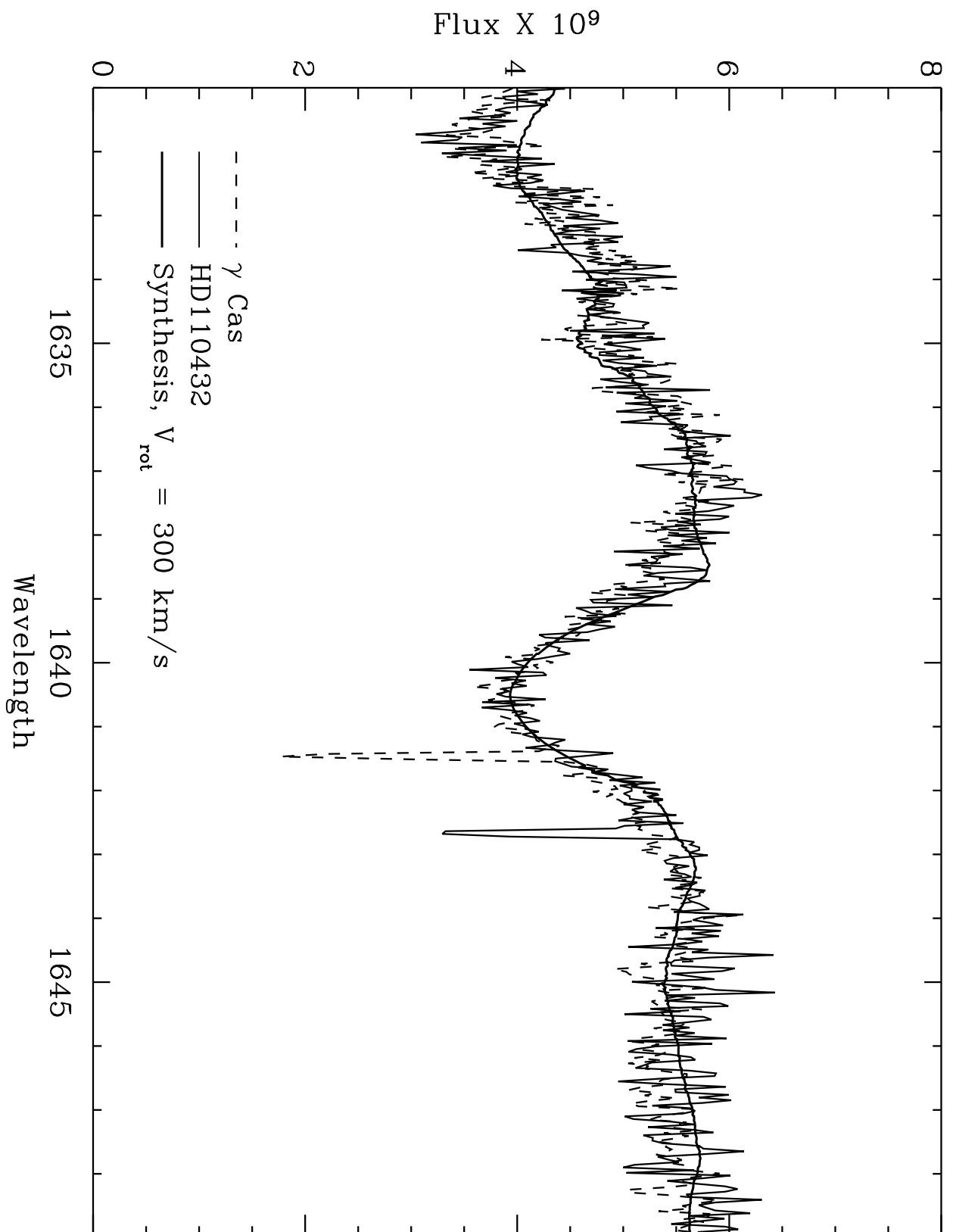
Fig. 8.— Grayscale difference spectra of the He I 6678 Å line of HD 110432 on the dates indicated. Starting times are 23:00 U.T. and 23:15 U.T., respectively. Limits of ± 300 km s⁻¹ on the line profile are indicated as the approximate extent of the rotationally broadened component of the absorption profile.

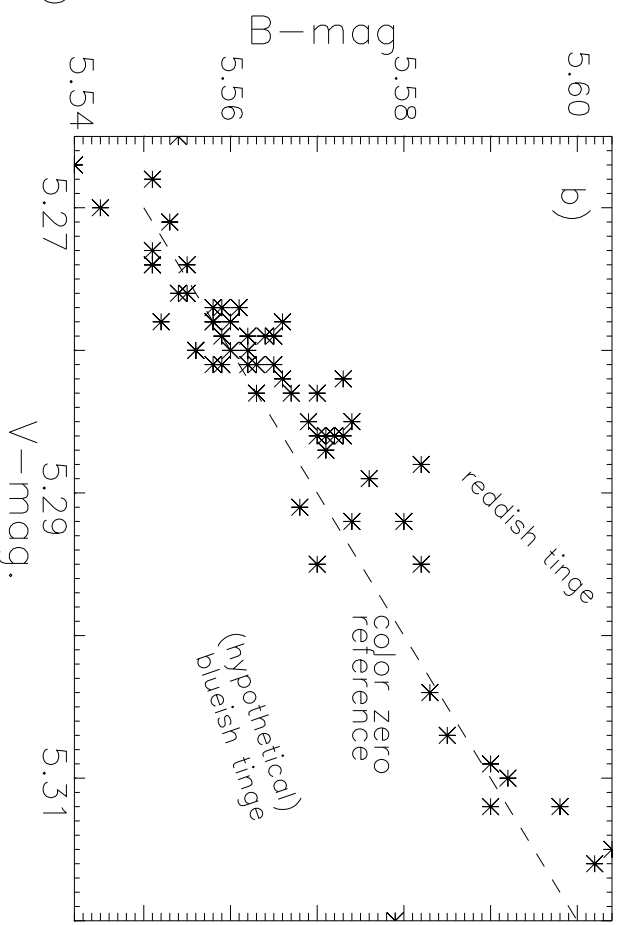
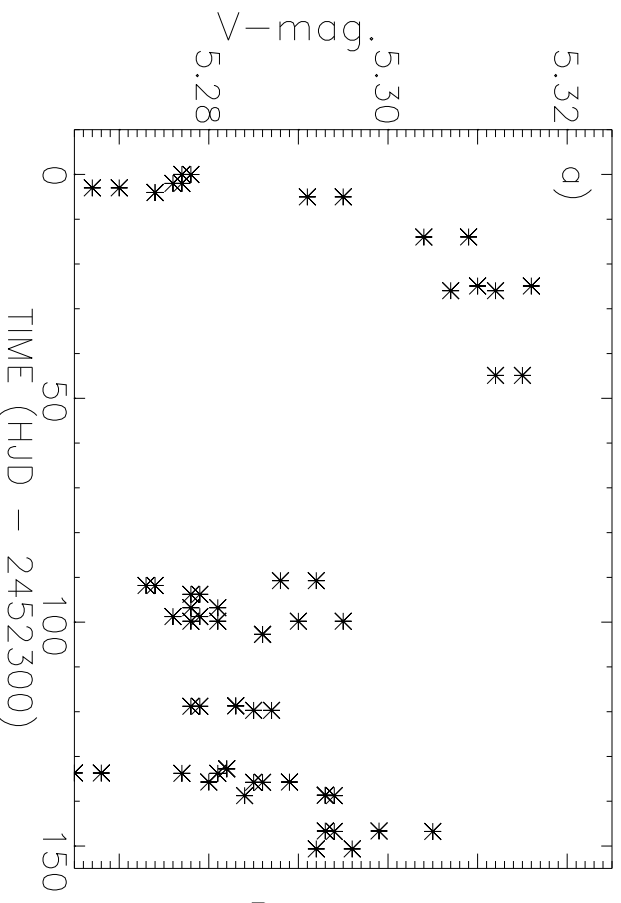
Fig. 9.— Montage of HeI and FeII line emission profiles from the mean spectra of the January and February, 2005 monitoring campaigns. The dashed and dotted vertical lines denote the mean separation of the V and R emission lobes for the January and February datasets.

Table 1: Emission Line Identifications and Strengths

Ion	Wavelength (vac.)	χ (eV)	Observed EW (mÅ)	Computed EW (mÅ)
S II	4524.68-.94	15.5		
Fe II	4555.89	2.8		
Fe II	4583.84	2.8	-0.182±.032	-0.182
Fe II	4629.34	2.8	-0.076±.011	-0.058
Fe II	4666.76	2.8	-0.080±.015	-0.056
Fe II	4923.93	2.9	-0.101±.004	-0.103
Fe II	5018.44	2.9	-0.252±.026	-0.312
Fe II	5169.03	2.9	-0.264±.008	-0.258
Fe II	5197.58	3.3	-0.150±.007	-0.137
Fe II	5234.62	3.2		
Fe II	5276.60	3.2	-0.164±.028	-0.190
Fe II	5284.07	10.5		
Fe II	5316.62	3.2	-0.236±.030	-0.217
S II	5362.87	3.2	-0.122±.002	-0.090
Fe II	5534.89	10.5		
He I	5875.62	21.1	-0.304±.004	-0.300
He I (Feb.)	5876.62	21.1	-0.361±.004	
Fe II	6247.55	3.9		
Fe II	6317.98	5.5	-0.161±.051	-0.043
Si II	6347.11	8.1		
Fe II	6456.38	3.9	-0.145±.024	-0.118
He I	6678.15	21.2	-0.146±.003	-0.150
He I (Feb.)	6678.15	21.2	-0.199±.013	

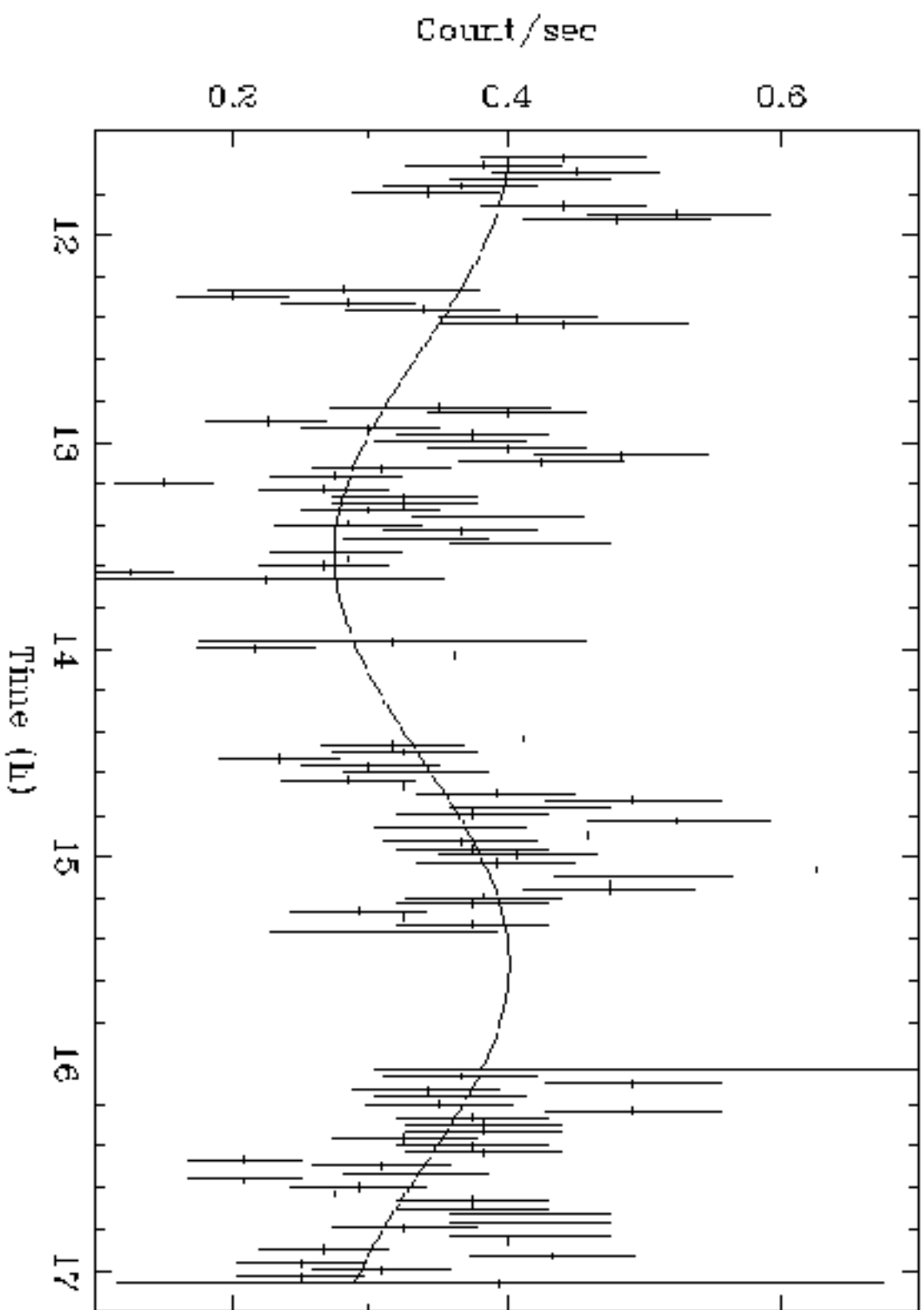




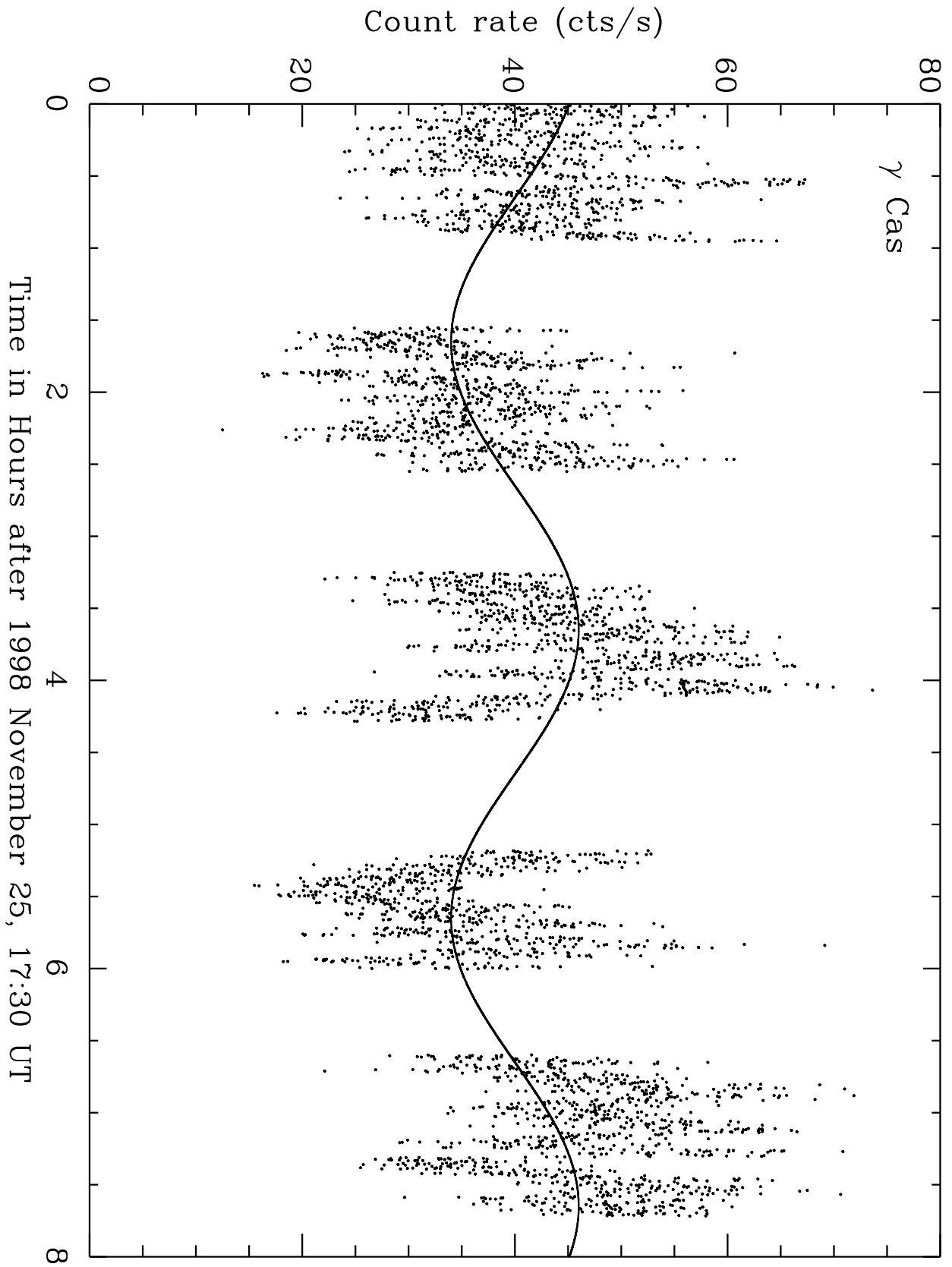


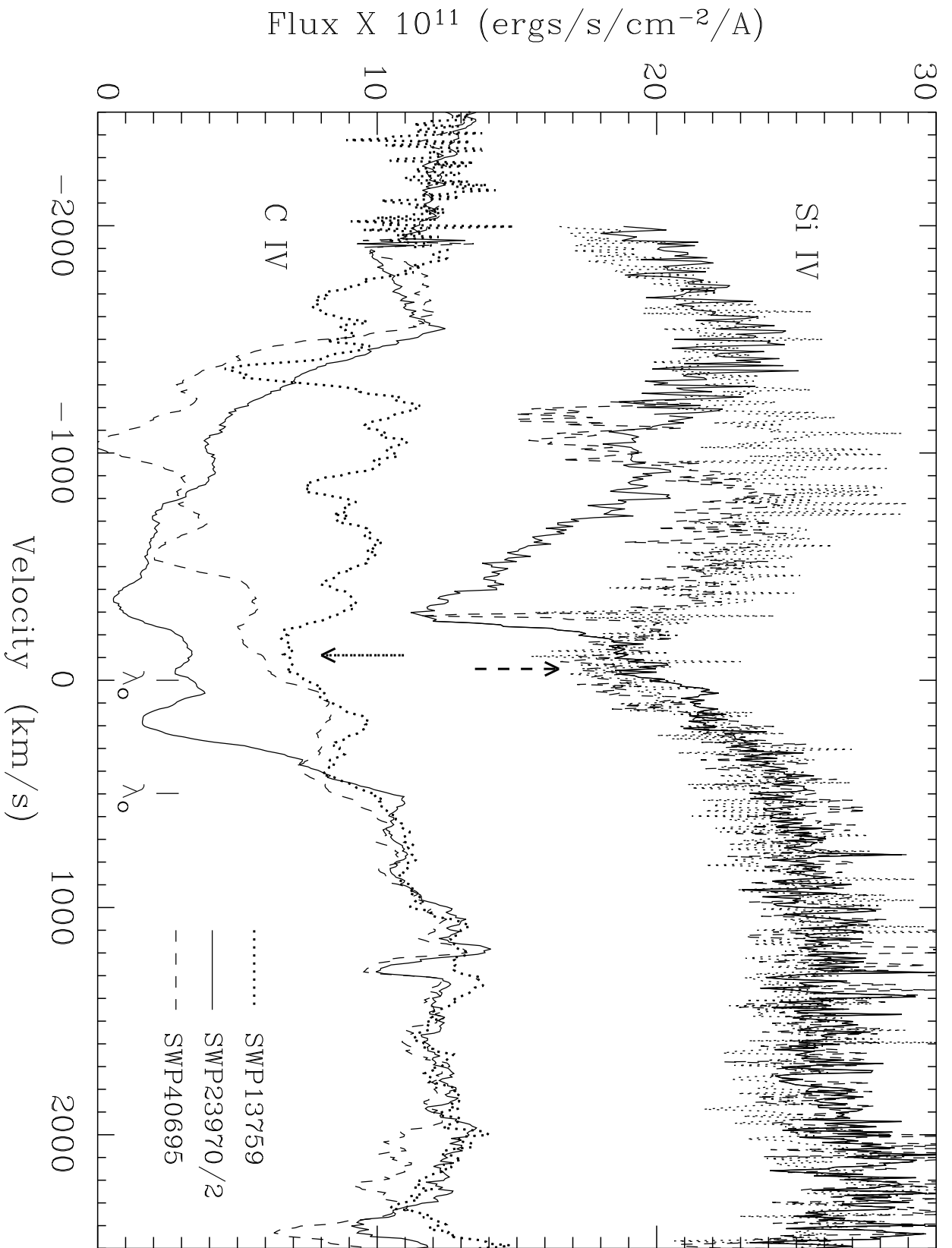
HD 110432

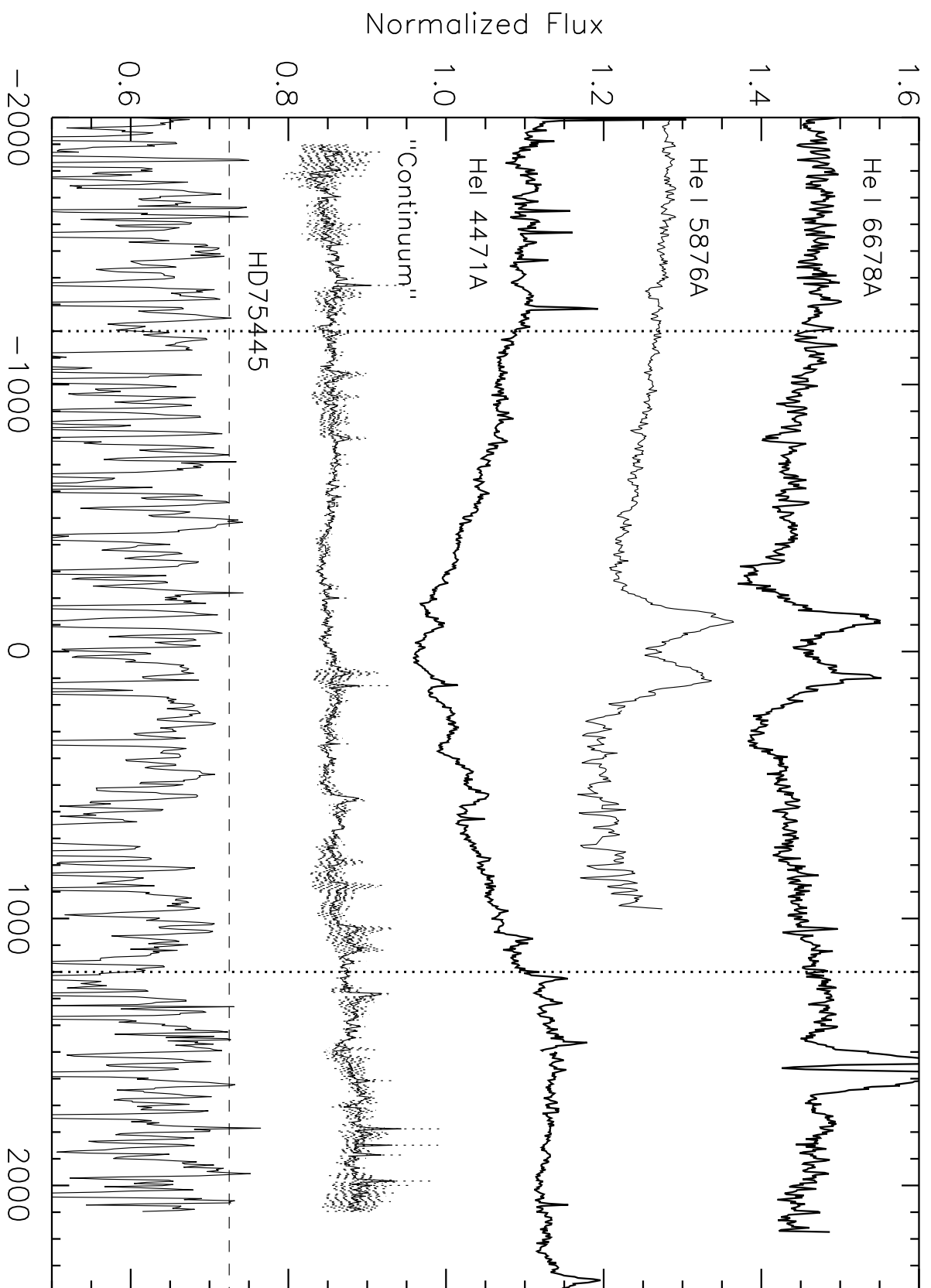
Bin time: 120.0 s



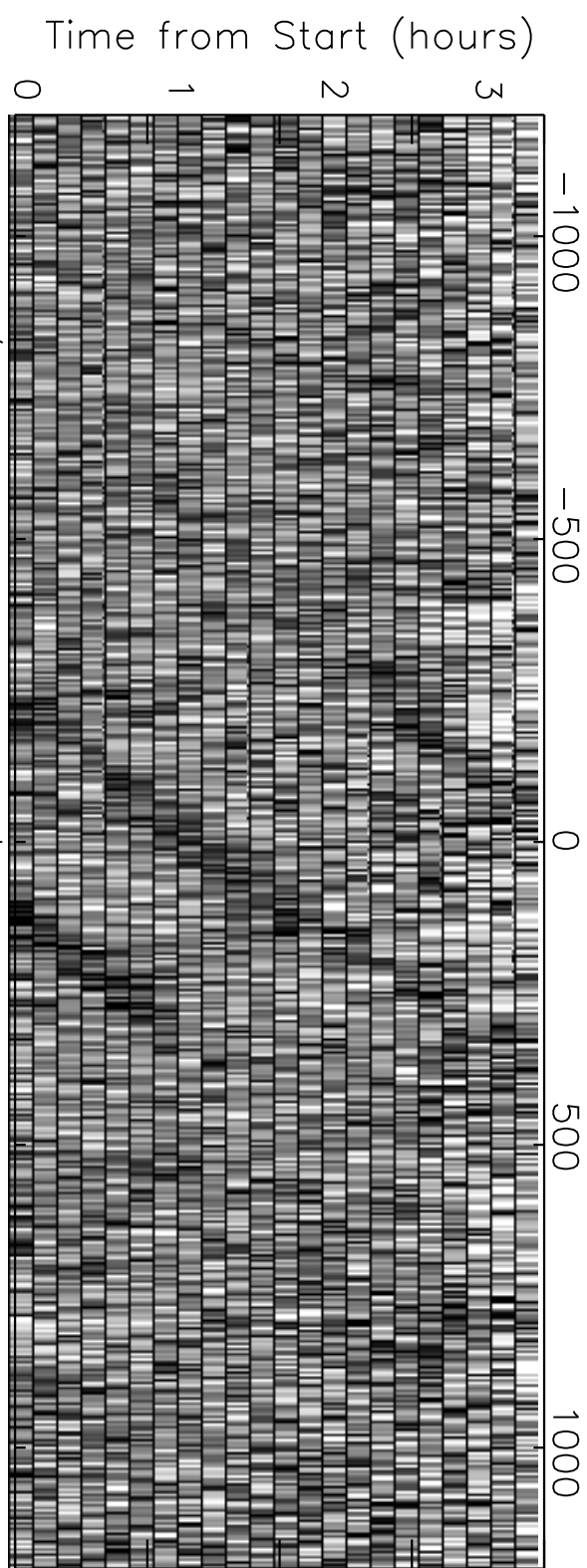
Start Time 10402 11.37.40.005 Stop Time 10402 17. 3.40.005



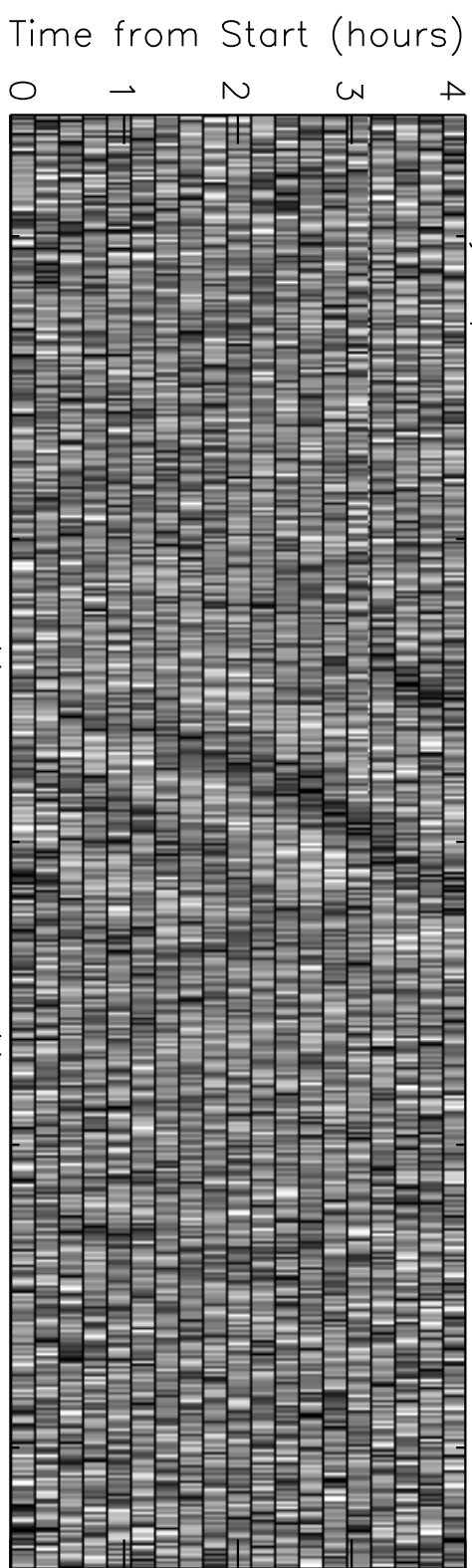




January 26/27, 2005



a)



b)

Velocity (km/s)

